PROCEEDINGS OF SPIE

SPIEDigitalLibrary.org/conference-proceedings-of-spie

Commissioning, on sky performance and first operations of JPCam, a 1.2 Gpixel camera for the wide-field 2.6m Javalambre Survey Telescope

A. Marín-Franch, S. Rueda-Teruel, G. López-Alegre, C. Íñiguez, H. Vázquez Ramió, et al.

A. Marín-Franch, S. Rueda-Teruel, G. López-Alegre, C. Íñiguez, H. Vázquez Ramió, A. Ederoclite, R. Bello Ferrer, M. Royo Navarro, J. M. Casino-Martín, D. Lozano-Pérez, E. L. Molina-Ibáñez, F. Rueda-Teruel, A. Yanes-Díaz, A. del Pino, C. López-Sanjuan, A. J. Cenarro, D. Cristóbal-Hornillos, A. Hernán-Caballero, M. Moles, J. Varela, S. Bielsa, S. Chueca, M. Domínguez, D. Garcés, N. Martínez, J. Muñoz, H. Rueda, I. Soriano, J. Castillo, T. Civera, J. Hernández, A. López-Sainz, A. Moreno-Signes, D. Muniesa-Gallardo, K. Taylor, F. Santoro, J. Cepa, C. Fermino, M. Bastable, G. Haddow, I. Palmer, M. Robbins, C. Simpson, A. Spatola, H. Sweeney, C. Tatard, M. Watkins, U. Brauneck, J. M. Casalta, R. Abramo, J. Alcaniz, N. Benítez, S. Bonoli, S. Carneiro, R. Dupke, C. Mendes de Oliveira, L. Sodré Jr., J. M. Vílchez, "Commissioning, on sky performance and first operations of JPCam, a 1.2 Gpixel camera for the wide-field 2.6m Javalambre Survey Telescope," Proc. SPIE 12184, Ground-based and Airborne Instrumentation for Astronomy IX, 121840M (29 August 2022); doi: 10.1117/12.2627024

SPIE.

Event: SPIE Astronomical Telescopes + Instrumentation, 2022, Montréal, Québec, Canada

Commissioning, on sky performance and first operations of JPCam, a 1.2 Gpixel camera for the wide-field 2.6m Javalambre Survey Telescope

A. Marín-Franch[a], S. Rueda-Teruel[b], G. López Alegre[b], C. Iñiguez[b], H. Vázquez Ramió[a], A. Ederoclite[a], R. Bello[b], M. Royo-Navarro[b], J. M. Casino-Martín[b], D. Lozano-Pérez[b], E. L. Molina-Ibáñez[b], F. Rueda-Teruel[b], A. Yanes-Díaz[b], A. del Pino[b], C. López-Sanjuan[a], A. J. Cenarro[a], D. Cristobal-Hornillos[a], A. Hernán-Caballero[b], M. Moles[a], J. Varela[a], S. Bielsa de Toledo[b], S. Chueca[b], M. Domíngez-Martínez[b], D. Garcés-Cubel[b], N. Martínez-Olivar[b], J. Muñoz-Maudos[b], H. Rueda-Asensio[b], I. Soriano-Laguía[b], J. Castillo[b], T. Civera[b], J. Hernández-Fuertes[b], A. López-Sáinz[b], A. Moreno-Signes[b], D. Muniesa-Gallardo[b], K. Taylor[c], F. Santoro[d], J. Cepa[e, f], C. Fermino[g], M. Bastable[h], G. Haddow[h], I. Palmer[h], C. Simpson[h], A. Spatola[h], H. Sweeney[h], C. Tatard[h], M. Watkins[h], U. Brauneck[i], J. M. Casalta[j], R. Abramo[k], J. Alcaniz[l], N. Benítez[m], S. Bonoli[n, o], S. Carneiro[p], R. Dupke[q], C. Mendes de Oliveira[r], L. Sodré Jr[r], and J. Vilchez[m]

[a]Centro de Estudios de Física del Cosmos de Aragón (CEFCA), Unidad Asociada al CSIC, Plaza San Juan 1, 44001 Teruel, Spain
[b]Centro de Estudios de Física del Cosmos de Aragón (CEFCA), Plaza San Juan 1, 44001 Teruel, Spain
[c]Instruments4, CA 91011, USA
[d]Magdalena Ridge Observatory/New Mexico Tech, 801 Leroy Place, Socorro, NM, 87801, USA
[e]Departamento de Astrofísica, Universidad de La Laguna, 38206 La Laguna Tenerife, Spain
[f]Instituto de Astrofísica de Canarias, 38200 La Laguna, Tenerife, Spain
[g]EFE Tecnologias Industriais, Araraquara, São Paulo, Brazil
[h]Teledyne-E2V (UK), 106 Waterhouse Lane, Chelmsford, Essex, CM1 2QU, UK
[i]Schott Suisse SA, Rue Galilée 2, CH-1401 Yverdon-les-Bains, Switzerland
[j]SENER Aeroespacial S.A., Spain
[k]Instituto de Física, Universidade de São Paulo, Rua do Matão 1371, CEP 05508-090, São Paulo, Brazil
[l]Observatório Nacional, Ministério da Ciencia, Tecnologia, Inovação e Comunicações, Rua General José Cristino, 77, 20921-400, Rio de Janeiro, RJ, Brazil
[m]Instituto de Astrofísica de Andalucía CSIC, Apdo 3004, 18080 Granada, Spain
[n]Donostia International Physics Center (DIPC), Manuel Lardizabal Ibilbidea, 4, San Sebastián, Spain
[o]Ikerbasque, Basque Foundation for Science, 48013 Bilbao, Spain
[p]Instituto de Física, Universidade Federal da Bahia, 40210-340 Salvador, BA, Brazil
[q]Observatório Nacional, Ministério da Ciencia, Tecnologia, Inovação e Comunicações, Rua General José Cristino, 77, São Cristóvão, 20921-400 Rio de Janeiro, Brazil
[r]Departamento de Astronomia, Instituto de Astronomia, Geofísica e Ciéncias Atmosféricas, Universidade de São Paulo, São Paulo, Brazil

Further author information: (Send correspondence to A.M.F.)
A.M.F.: E-mail: amarin@cefca.es, Telephone: +34 978 221 266

Ground-based and Airborne Instrumentation for Astronomy IX, edited by Christopher J. Evans, Julia J. Bryant, Kentaro Motohara, Proc. of SPIE Vol. 12184, 121840M
 · 0277-786X · doi: 10.1117/12.2627024

ABSTRACT

Commissioning results, on-sky performance and first operations of the Javalambre Panoramic Camera (JPCam) are presented in this paper. JPCam is a 1.2 Gpixel camera deployed on the 2.6m, large field-of-vie Javalambre Survey Telescope (JST250) at the Observatorio Astrofísico de Javalambre. JPCam has been conceived to perform J-PAS, a photometric survey of several thousand square degrees of the northern sky in 56 optical bands, 54 of them narrow-band filters (145 Å FWHM), contiguous and equi-spaced between 370 and 920nm, producing a low resolution photo-spectrum of every pixel of the observed sky, hence promising crucial breakthroughs in Cosmology and galaxy formation and evolution. JPCam has been designed to maximize field-of-view and wavelength coverage while guaranteeing a high image quality over the entire focal plane. To this aim, JPCam is equipped with a mosaic of 14 9.2k x 9.2k, 10µm pixel, low noise detectors from Teledyne-E2V, providing a FoV of 4.1 square degrees with a plate scale of $0.2267''$/pix. In full frame mode, camera electronics allows read times of 10.9s at 633kHz read frequency (16.4s at 400kHz) with a readout noise of $5.5e^-$ ($4.3e^-$). Its filter unit admits 5 filter trays, each mounting 14 filters corresponding to the 14 CCDs of the mosaic and allowing all the J-PAS filters to be permanently installed. To fully optimize image quality, position of JST250 secondary mirror and JPCam focal plane are maintained optically aligned by means of two hexapod systems. To perform this task, JPCam includes 12 auxiliary detectors, 4 for autoguiding and 8 for image quality control through wavefront sensing.

Keywords: J-PAS, Instrumentation, CCD Camera, CCD mosaic, wide field, narrow-band filters, JPCam, Observatorio Astrofísico de Javalambre, OAJ

1. INTRODUCTION

The Javalambre Physics of the Accelerated Universe Astrophysical Survey[1,2] (J-PAS[*]) is a Spanish-Brazilian collaboration to conduct an innovative photometric all-sky survey of thousands of square degrees of the Northern Sky. It will observe through a set of 54 contiguous, narrow band optical filters (145 Å width each, placed ~ 100 Å apart), plus two broad band filters at the blue and red sides of the optical range to reach aperture magnitude depth of AB = 22.5 — 23.5, depending on the wavelength (5σ in $3''$ aperture). Adjacent filters have a certain overlap ensuring a spectral measurement over the whole spectrum from about 320nm to over 1050nm with 56 different spectral channels without any significant modulation as a function of the redshift. Although it has been designed and optimized to achieve 0.3 % relative error photometric redshifts (photo-zs) for tens of millions of galaxies, enabling measurements of the cosmological baryonic acoustic oscillation (BAO) signal across a relatively wide range of cosmic epochs, the use of the narrow band filters makes J-PAS to be equivalent to a low resolution Integral Field Unit (IFU) of the Northern Sky, hence providing the spectral energy distribution of every pixel of the sky and, ultimately, a 3D image of the Northern Sky with an obvious wealth of potential astrophysical applications. This makes J-PAS a highly versatile project that will produce a unique legacy-value data set for a broad range of astrophysical studies of solar-system bodies, stars, galaxies, and cosmology.

The survey will be carried out at the Observatorio Astrofísico de Javalambre (OAJ) using the dedicated 2.55m Javalambre Survey Telescope (JST250), characterized by a very large Field of View (3 degree diameter), and the Javalambre Panoramic Camera (JPCam), a 1.2 Gpixel camera spanning an area of 4.1 square degrees with its 14 large format CCD mosaic.

1.1 Observatorio Astrofísico de Javalambre - OAJ

The Observatorio Astrofísico de Javalambre[3] (OAJ[†]) is an astronomical infrastructure conceived to carry out large sky surveys from the Northern hemisphere with dedicated telescopes of unusually large field-of-view (FoV). The OAJ is located at the Pico del Buitre of the Sierra de Javalambre, in Teruel, Spain. The site, at an altitude of 1957 m avobe sea level, has excellent astronomical characteristics in terms of median seeing ($0.71''$ in V band, with a mode of $0.58''$), fraction of clear nights (53 % totally clear, 74% with at least a 30% of the night clear) and darkness, with a typical sky surface brightness of $V \sim 22\,\mathrm{mag}\,''^{-1}$ at zenit during dark nights, a feature quite exceptional in continental Europe. Full details about the site testing of the OAJ can be found in.[4]

[*] http://j-pas.org
[†] http://oajweb.cefca.es

The observatory is fundamentally organized around two telescopes, the Javalambre Survey Telescope (JST250), a 2.55 m telescope with a FoV of 3 deg diameter, and the Javalambre Auxiliary Survey Telescope (JAST80), a 0.83 m telescope with a FoV of 2 deg diameter. The two telescopes are equipped with panoramic instrumentation for direct imaging that allows to carry out photometric surveys with an ample spectrum of key astrophysical applications. The first defined surveys that are being carried out with the OAJ telescopes are the J-PAS and the Javalambre Photometric Local Universe Survey (J-PLUS[‡]), aimed to cover thousands of square degrees of the sky visible from Javalambre with an specific set of 56 narrow-band, contiguous, optical filters (J-PAS) and 12 broad-, medium-, narrow-band optical filters (J-PLUS).

The OAJ was planned from scratch to be a fully automated astronomical observatory to perform efficient operations from a global point of view for the whole observatory processes, maximizing observatory operations performance, achieving scientific objectives, maintaining quality requirements but also minimizing resources, materials and human interaction.

Apart from the telescopes, scientific instrumentation, Global Observatory Control System (GOCS) and general infrastructure, the OAJ also includes the data center *Unidad de Procesado y Archivo de Datos*[5] (UPAD) with capacity to provide reduced and calibrated data on a quasi-real time basis and to archive and allow external access to the whole scientific community to images, data and UPAD generated catalogues.

The definition, design, construction, exploitation and management of the observatory and the data produced at the OAJ are responsibility of the Centro de Estudios de Física del Cosmos de Aragón (CEFCA[§]). The OAJ project started in March 2010, mostly funded by the *Fondo de Inversiones de Teruel*, a programme supported by the local Government of Aragón and the Government of Spain, and is essentially completed since 2015. In October 2014, the OAJ was awarded with the recognition of Spanish ICTS (*Infraestructura Científico Técnica Singular*) by the Spanish Ministry of Economy and Competitiveness.

1.2 Javalambre Survey Telescope - JST250

The main telescope at the OAJ is the Javalambre Survey Telescope[6] (JST250), an innovative Ritchey-Chrétien-like, alt-azimuthal, large-etendue telescope with an aperture of 2.55 m and 3 deg diameter FoV. JST250 is the telescope dedicated to the development of the J-PAS survey. The focal plane of JST250 corresponds to a Cassegrain layout. The primary and secondary mirrors have hyperbolic aspheric surfaces. The effective collecting area of JST250 is 3.75 m^2, yielding an etendue of 26.5 m^2 deg^2. Motivated by the need of optimizing the etendue, JST250 is a very fast optics telescope (F#3.5) with a plate scale of 22.67″/mm.

The optical design has been optimized to provide a good image quality in the optical spectral range (330-1100 nm) all over the 48 cm diameter focal plane (7 deg^2). The polychromatic as-built EE50 image quality is better than 6.21 μm (radius). To guarantee the above image quality over the entire focal plane, the JST250 includes a unique field corrector of 3 lenses of fused silica, with 4 aspherical surfaces and diameters ranging from 62 to 51 cm.

Because of its fast optics, JST250 is a very compact telescope. The distance between its primary and secondary mirrors is only 2.2 m. This fact allows the dome to be compact too, having a diameter of approximately 13 m. JST250 weights about 45000 kg. The back focal distance of JST250 is 318 mm. It is able to support instruments of up to 1500 kg at 750 mm from the mounting flange. The instrumentation is supported by the rotator that compensates for field rotation. In order to guarantee an optimal image quality all over the entire FoV of the telescope, M2 is supported and controlled by a hexapod actuator. This allows to perform fine corrections of the M2 position in piston, x-y decentring and tip/tilt to compensate temperature changes and/or mechanical flexures at different telescope pointings. Table 1 illustrates a summary of the main technical characteristics of JST250.

[‡] http://www.j-plus.es
[§] http://www.cefca.es

Table 1. Main technical characteristics of the JST250 telescope

Mount:	Altazimuthal
Optical configuration:	Ritchey Chrétien modified, equipped with a field corrector and rotator
M1 diameter:	2.55 m
Field corrector:	3 aspherical lenses
Effective collecting area:	3.75 m^2
Focus:	Cassegrain
F#:	3.5
Focal length:	9098 mm
Plate scale:	22.67″ mm^{-1}
FoV (diameter)	3.0 deg
Etendue:	26.5 $m^2 deg^2$
EE50 (diameter, as-built)	12.5 μm
EE80 (diameter, as-built)	25 μm

2. JPCAM, A 1.2GPIX CAMERA FOR THE J-PAS SURVEY

The main scientific instrument of the JST250 is the Javalambre Panoramic Camera[7,8] (JPCam, Figure 1), a 1.2 Gpixel camera conceived to perform J-PAS. The definition and procurement of JPCam was lead by CEFCA and the J-PAS Collaboration. The instrument has been funded by a consortium of several institutions from Spain (CEFCA and IAA-CSIC) and Brazil (ON, IAG/USP, and CBPF).

JPCam has been designed to maximize FoV and wavelength coverage while guaranteeing a high image quality over the whole focal plane and providing low read noise images. To this aim, JPCam is equipped with a mosaic of 14 CCD290-99 9.2k x 9.2k, 10 μm pixel, low noise detectors from Teledyne-E2V, providing an effective FoV of 4.1 deg^2 with a plate scale of 0.23″/pix. In full frame mode, camera electronics allows read times of 10.9s at 633kHz read frequency (16.4s at 400kHz) with a readout noise of 5.5e^- (4.3e^-). Its filter unit admits 5 filter trays, each mounting 14 filters corresponding to the 14 CCDs of the mosaic.

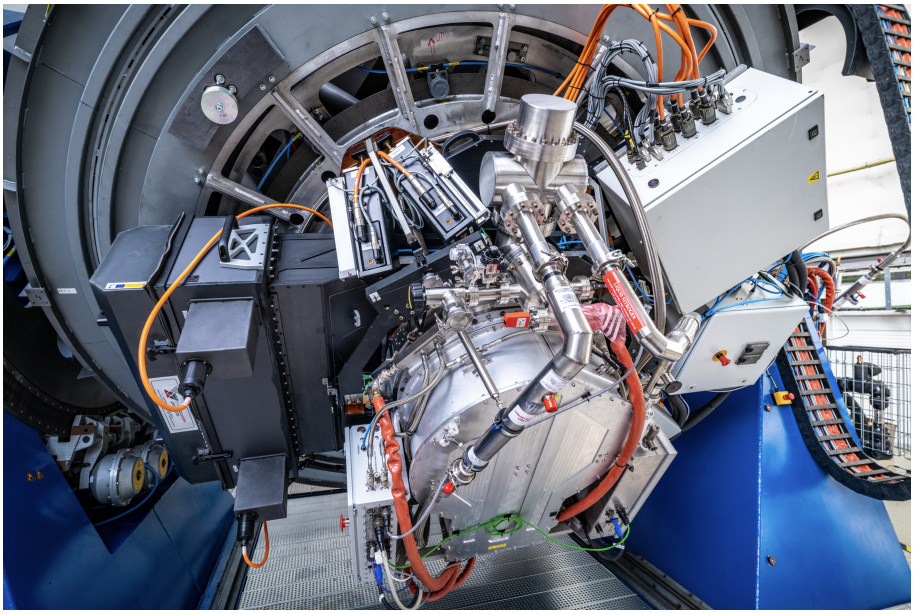

Figure 1. JPCam fully integrated at the Cassegrain focus of the JST250 telescope.

Table 2. Main technical characteristics of the JPCam

CCD format	$14 \times 9216 \times 9232$ pix, $10\,\mu$m pix^{-1}
	1.2 Gpix camera
Pixel scale	$0.2265''$ pix^{-1}
FoV	4.1 deg^2
	(14×) 0.56 deg × 0.53 deg
Read out time (633kHz)	10.9 s (full frame) − 6.1 s (2x2 binning)
Read out noise (633kHz)	5.5 e$^-$ (RMS)
Read out time (400kHz)	16.4 s (full frame) − 8.9 s (2x2 binning)
Read out noise (400kHz)	4.3 e$^-$ (RMS)
Gain	2.274 $e^- ADU^{-1}$
Minimum exposure time	0.1 s
Exposure homogeneity	1 ms
Full well	> 125 000 e$^-$
QE	40% (350nm)
	86% (400nm)
	93% (500nm)
	93% (650nm)
	61% (900nm)
CTE	>99.9990%
Dark current	0.001 e$^-$ pix^{-1} s^{-1}
Number of filters	70

Because of the large FoV and fast optics, and to ensure optimum image quality, the JST250 secondary mirror and the JPCam focal plane are actively controlled with two hexapod actuators, the M2 hexapod and the JPCam Actuator System. This allows to perform fine corrections of the secondary mirror and instrument positions in piston, x-y decentering and tip/tilt to compensate for temperature changes and/or mechanical flexures at different telescope and instrument orientations. This is done through a wave-front curvature sensing and analysis technique developed at CEFCA[9] that computes the optimal hexapod position for a given temperature and telescope pointing (see Section 2.5). To support this task, JPCam includes 12 auxiliary detectors, 4 for autoguiding and 8 for image quality control through wave-front curvature sensing.

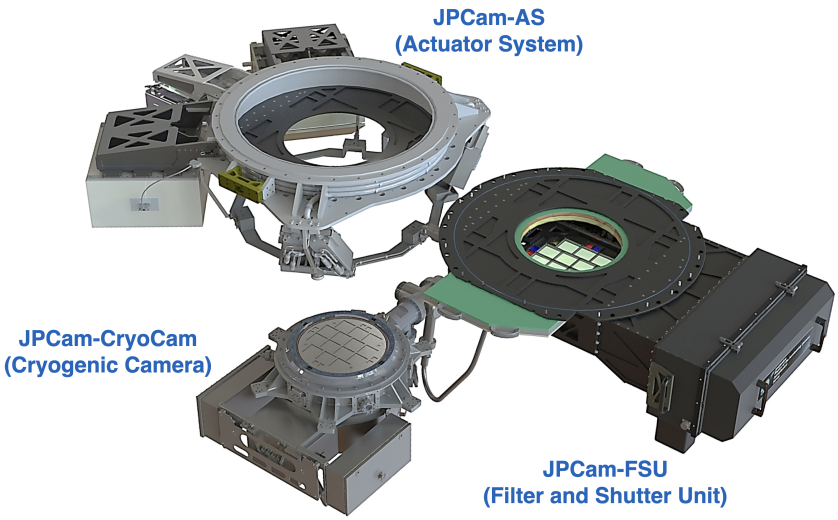

Figure 2. Model view of the three JPCam main subsystems.

The instrument has a total mass of 1495kg, and it is broken down into three main subsystems: cryogenic camera (CryoCam, Section 2.1), Filter and Shutter Unit (FSU, Section 2.2) and Actuator System (AS, Section 2.3). Table 2 summarises JPCam main characteristics and Figure 2 shows the instrument 3D model design with its three main subsystems deployed.

2.1 Cryogenic camera

The JPCam 1.2 GPix Cryogenic camera[10] (Figure 3) comprises a powered dewar window, the 14 scientific CCD mosaic and their associated controllers, the cooling and vacuum systems and the image acquisition electronics and CCD control software. The science CCD mosaic is complemented with 12 auxiliary detectors, 4 for auto-guiding (AG) and 8 for wave-front sensing (WFS) and image quality control. The proximity drive electronics achieves total system level noise performance of 5.5e- from the 224-channel CCD system when reading out the system at 633kHz. This allows a read out of the whole CCD mosaic in 10.9s (full frame) of 6.1s (2x2 binning). The camera includes PLC (Programmable Logic Computer) control electronics for the cooling and vacuum systems. The CryoCam has been supplied by Teledyne-E2V (Chelmsford, UK).

The heart of the camera is its focal plane mosaic, composed by a total of 26 CCDs of three different types:

- 14 × CCD290–99 (Science CCDs). These are large format 9.2k x 9.2k, 10µm pixel, non-inverted, full frame, deep depletion, Astro multi-2 CCDs. Each CCD has 16 outputs for low readout time peak QE over 90% over a wide spectral range. Differential outputs are available.
- 8 × CCD44–82 (Wave-front CCDs, WFS). 2048 X 2048 Frame-transfer.
- 4 × CCD47–20 (Auto-guide CCDs, AG). 1024 X 1024 Frame-transfer

The focal plane array is integrated on a 600 mm diameter aluminium cold plate and integrates light baffles. The flatness of the focal plane is one of the most challenging and important requirements on JPCam as it directly impacts on final image quality. The achieved science CCD mosaic flatness is 27m peak-to-valley, measured at operating temperature.

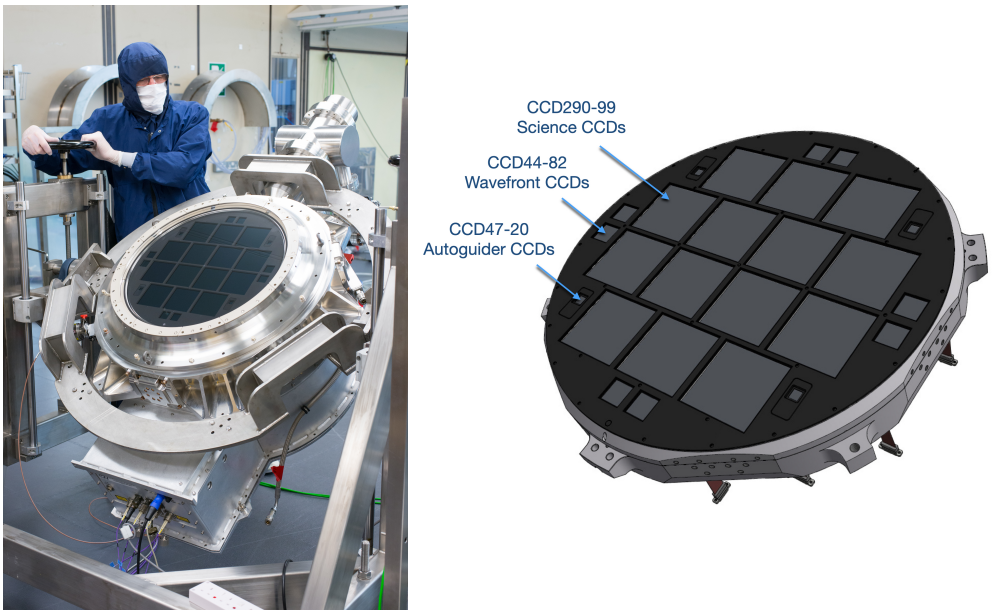

Figure 3. Left: JPCam Cryogenic camera during final assembly and tests at Teledyne-E2V premises. Massive focal plane can be observed. Right: 3D model of the focal plane of the JPCam with its 14 science plus 12 auxiliary CCDs.

The Cryogenic camera includes readout electronics for all the CCDs. The system includes a total of 22 CCD drive modules, each one with 16 low noise 16bit 100MHz DCDS analogue input chains and capacity to store

the 81 MPixel image data in on-board DDR2 SDRAM Framestore. The drive modules provide low noise bias voltages to the CCDs, performs clock waveform generation and outputs the reconstructed image via a single high speed serial LVDS link (carried over HDMI cables). Overall, the camera electronics provide power and data handling electronics, include 4 optical CameraLink interfaces to camera for command and data telemetry, over 50 FPGAs to handle the 2.4 GBytes of data per frame. It offers digital CDS (Correlated Double Sampling) read-out. Electronics include a glycolated water cooling system. The data from the sensors is gathered in the Detector Electronics Box and transmitted via Camera Link ports to a dedicated image server. Two fibre optic channels are used to transmit the Science CCD data to reduce data transmission times.

The camera is cryogenically cooled using a continuous flow cryostat system. Two LN2 tanks, mounted on the telescope's fork, feed the cryostat through routing of flexible cooling lines via the telescope cable wraps, as required to accommodate both Cassegrain and altitude rotation. The focal plane is cooled thanks to its phase change LN2 cooling system. The cooling system has been designed to control the focal plane to a average temperature of -112^{o}C with a variation across the focal plane of better than $\pm 2.5^o$C and a stability of better than $\pm 0.5^o$C over the long periods of operation required. The chamber is evacuated to a level of 10^{-6} Torr using a serviceable turbo-pump and pressure will be maintained during operation using sorption pump material.

The camera dewar window is in fact the forth element of the JST250 field corrector, and together with the filters, it is part of the telescope optical design optimization. The window is a 580mm diameter and 29mm thick, weakly powered field-flattener with an 8mm distance between its inner surface and the focal plane mosaic. The dewar window has been supplied by Glyndwr Innovations Limited (St. Asaph, UK).

2.2 Filter and shutter unit

The Filter and Shutter Unit (FSU) comprises the filter tray exchange mechanism and the shutter. It has being designed by the J-PAS collaboration and Astro-EME, USA, and has been supplied by The Vacuum Projects (Spain) and Jaguar Precision Machine (USA). The massive 515mm aperture shutter is from Bonn-Shutter UG. The FSU has been designed to admit 5 filter trays, with 14 sicentifc plus 12 auxiliary filters per tray. This allows all J-PAS filters (see section 2.2.1) to be simultaneously installed on the camera so no night-to-night filter exchange is required. Figure 4 shows a filter tray during its integration at OAJ's clean room. On top of that, and aimed at maximising observing capabilities once open time becomes available to the astronomical community, three additional filter trays populated with Sloan g, Sloan r and Sloan i filters have been designed, manufactured and are available for JPCam at the OAJ.

The filter trays also have filter holders for broad-band filtering of the 12 auxiliary WFS and AG detectors. Each CCD will view only its corresponding filter avoiding optical cross-talk from their neighbours. With this configuration, the filters operate close to, but up-stream from, the dewar window in a fast converging beam.

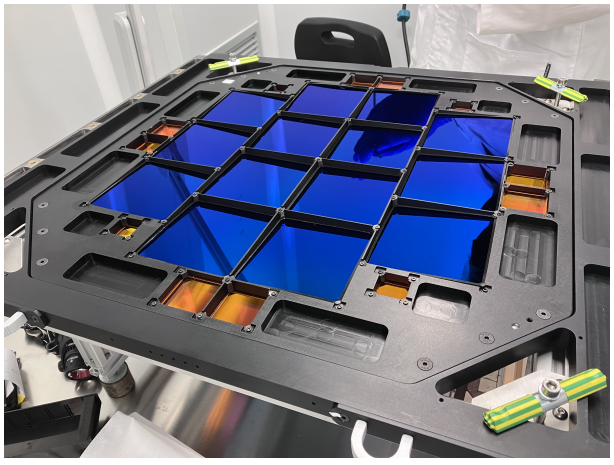

Figure 4. Sloan i JPCam filter tray during final assembly at the OAJ clean room.

The focal-plane of the JST250 telescope is non-telecentric. hence, and in order to retain the steepness of each intermediate-band filter bandpass profile and the uniformity of its wavelength centering, all science filters must be held in each tray so as to induce a differential tilt in each of the 14 filters of the mosaic, so that each filter is perpendicular to the chief ray at its centre. This amounts to a maximum tilt of $\sim 3.5^o$ for the outer filters. Furthermore, in order to minimize the peripheral vignetting of the CCD by its corresponding filter, the distance between filters and CCDs is required to be as close as practical. A nominal gap of 4.5mm between the filters and the dewar window has been chosen to allow for filter tray deployment and the necessity of moving the cryogenic camera with respect to the FSU with the Actuator System.

The FSU includes the motors, encoders, sensor system and control system needed for its operation. Filter trays are selectable remotely. The system has been designed to select and place a filter tray on the optical path in less than 40s. Additionally, and each filter tray is designed to be easily and manually removable and exchangeable from the FSU closed frame. Individual filters can be manually removable from their tray once the tray has been removed from the module.

The JPCam has a 515mm diameter aperture. It is a 'two-curtain' shutter that guarantees an homogeneous illumination of the focal plane. It allow for exposures as short as 10ms with an exposure uniformity better than 1ms over the full FoV.

Finally, in order to prevent frost and/or condensation from forming on the large (about 550mm diameter) dewar window, the FSU is sealed and slightly over-pressured with dry air. The over-pressure is actively controlled to a 0.4mbar level and, to avoid possible damage on the telescope wide field corrector and dewar large lenses, it includes a safety relief valve system that is triggered at 1.4mbar.

2.2.1 J-PAS filter system

JPCam is equipped with the J-PAS filter system, a set of 54 contiguous, narrow band optical filters (145 Å width each, placed ~ 100 Å apart), plus two broad band filters at the blue and red sides of the optical range that effectively delivers a low-resolution spectra ($R \sim 60$) for every observed object observed. It has been designed and optimized to achieve 0.3 % relative error photometric redshifts (photo-zs). Beyond the specified theoretical filter transmission curves, whose definition is exclusively driven by the main scientific goals, additional functional requirements are influenced by the telescope and instrument opto-mechanical designs. Some of the most demanding requirements are: filter's physical dimension (101.7 mm $\times$ 96.5 mm), central wavelength (CW) uniformity across the filter's usable area (CW varies less than $\pm$ 0.2% of each filter's CW), high band-pass transmission and flatness (higher than 90%, except for the bluest filters, with a flatness better than 5% p-t-v), out of band blocking (OD5 from 250 to 1050 nm) and filter-to-filter continuity (overlap at transmissions higher that 75%).

Table 3. filter system main characteristics.

Filter #	Filter name	Central Wavelength [Å]	FWHM [Å]
1	*J*0348	3485	495
2	*J*0378	3785	155
3	*J*0390	3900	145
4	*J*0400	4000	145
5	*J*0410	4100	145
...	...	...	...
54	*J*0900	9000	145
55	*J*0910	9100	145
56	*J*1007	10075	*High-pass filter*

In order to achieve these requirements, each J-PAS filter consist a sandwich of either two or three optical color glasses and B270 coated with interference filter and AR-coatings.[11–13] The filter layer systems consist of typically more than 150 layers with a few micrometers total thickness. The components have assembled with

an airspace (200μm): This design approach resulted on an optimum spectral behavior and excellent transmitted wavefronts. The J-PAS filters have been manufactured by SCHOTT Suisse SA (Switzerland). Table 3 list the main characteristics of the J-PAS filter set whereas Figure 6 shows the measured transmission curves of the 56 filters described above.

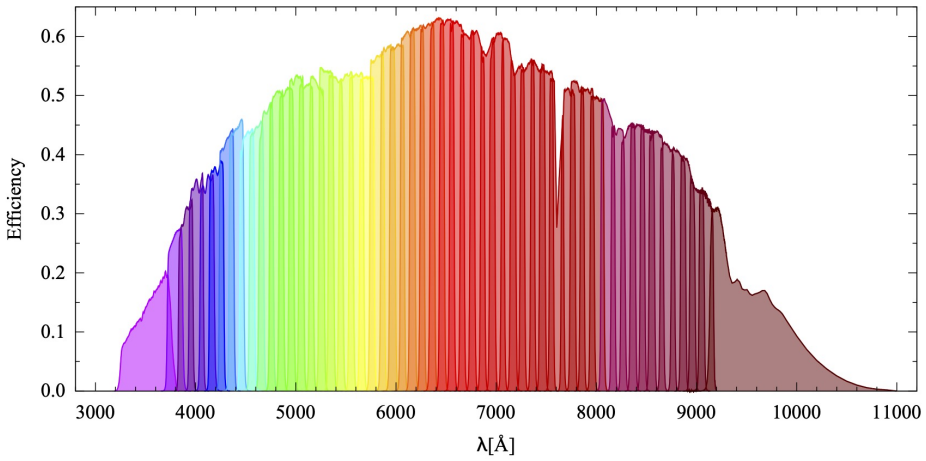

Figure 5. Measured transmission curves of the J-PAS filters (including effects of the CCD quantum efficiency, the entire optical system of the JST250 telescope and sky absorption.

It is worth mentioning that this unique filter set has been already used to observe 1 square degree of the sky (the so called mini-JPAS survey[2]). The data was taken using the JPAS-Pathfinder instrument, an interim, single CCD camera integrated at the JST250 telescope during years 2017-2019 before the arrival of JPCam.

The mini-JPAS represents the beginning of the J-PAS survey, demonstrating with on-sky data the scientific feasibility of the J-PAS novel observational approach. A public data release of mini-JPAS was made available in December 2019[¶]. Figure 6 shows a few photo-spectra examples for different classes of stars (A0 and K3V), an emission line galaxy and a quasar in the mini-JPAS field. The mini-JPAS public data release includes reduced images and a catalogue with more than 60.000 astronomical objects with more than 1.000 parameters per object. With 1 square degree observed, the mini-JPAS survey has demonstrated the potential of the J-PAS project definition and implementation. JPCam and JST250 represent a most efficient facility to perform large scale, multi-filter astronomical surveys. Several thousand square degrees of the northern sky will be observed, generating an unprecedented set of data with the potential of significant contributions to numerous areas of modern physics and astrophysics.

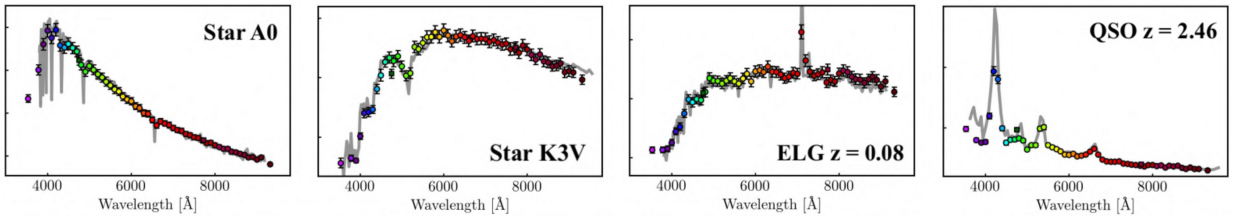

Figure 6. J-PAS photo-spectra of different classes of stars (A0 and K3V), an emission line galaxy and a quasar in the mini-JPAS field (coloured symbols) compared with the SDSS spectra (grey lines).

2.3 Actuator system

Because of the JST250 telescope's very wide FoV, combined with the confirmed excellence of the OAJ intrinsic site seeing, JPCam is required to fully optimise and maintain the image quality across the full focal plane at any

[¶] http://archive.cefca.es/catalogues/minijpas-pdr201912

pointing and observing condition. Optical analysis revealed that it is necessary, not only to guide the telescope and keep it optically aligned by adjusting the position of its secondary mirror, but also of the focal plane itself. To perform this task JPCam includes the actuator system,[14] an hexapod that is controlled thanks to the wave-front sensors included in the periphery of the cryogenic camera focal plane. The actuator system attaches the cryogenic camera to the telescope and provides the required focus and tip-tilt movement to compensate the telescope deformation produced by gravity and/or temperature variations. The actuator system has been supplied by Sener (Barcelona, Spain). It it provides a ±2mm stroke in focus and ±500″ in tip/tilt. Within these ranges, the actuator system is able to position the cryogenic camera, whose weight is about 600Kg, with and overall absolute focus accuracy of ±8μm and a relative focus accuracy of ±4μm (movements lower than 100μm). With respect to tip/tilt, the overall absolute accuracy is ±6″ and the relative tilt accuracy is ± 1″ (tilts lower than 20″).

The JPCam actuator system is controlled by a 6-axis Drive Motion Controller and amplifier that supports DC brushless and monitored through a set of linear, absolute encoders. The system has been designed to perform one movement in less than 2 seconds.

2.4 JPCam Control system

JPCam control system is based on two different technologies. On one side, the three main subsystems local control is based on a Beckhoff PLC control system. The cryogenic camera and the filter and shutter unit subsystems control makes use of Cx5020 versions of Beckhoff PLCs, and the actuator system, that is controlled by a Delta-Tau geobrick type controller at very low level, uses another PLC similar to that of the rest of subsystems to provide a uniform control layer. On the other side, the CCD control electronics, both for the images' acquisition and for their management, are controlled using its own gateway developed in cpp using an API provided by the cryogenic camera manufacturer. The gateway runs on a dedicated Dell R510 server, and uses two Matrox-brand frame grabber cards to exchange data with the detectors electronics box. All these low-level signals are stored in a Kepware OPC UA server that acts as the system's middleware. Finally, at the highest level, JPCam control system uses a set of displays designed at Ignition Inductive Automation, which act as a Human-Machine interface (HMI). Figure 7 shows JPCam the different control system layers.

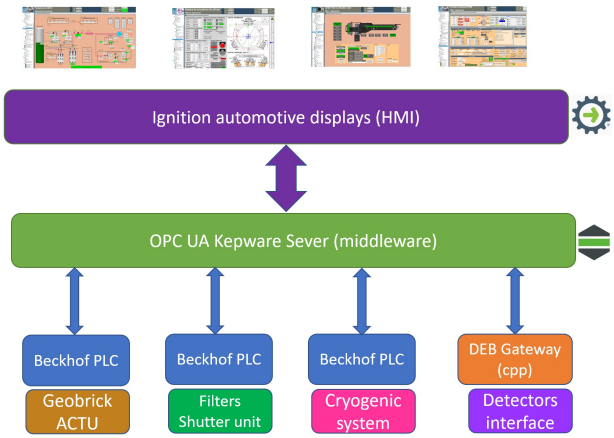

Figure 7. JPCam Control Layers.

2.5 Image quality Control system - OPAC

The very fast optics of large FoV telescopes of the OAJ, like JST250 and the JAST80 at the OAJ, makes the image quality (IQ) to be potentially very sensitive to small changes in temperature and in the gravity vector. Being aware of this circumstance, to maintain the IQ within tolerances during night operation CEFCA has developed an active optics software, namely `OPAC`,[6,9] based on wavefront curvature sensing techniques. This software is able to analyse intra- and extra-focal images at the OAJ telescope focal planes, interpreting this information in

terms of optical aberrations. Then, making use of empirical control laws that link such aberrations with the 3D positions of the secondary mirror (M2 hexapod) and the focal plane (JPCam Actuator System), the OPAC derives the corrections to be applied to the position of both systems to bring the IQ down to specifications.

The OPAC quantifies optical aberrations in terms of Zernike polynomials using the notation and equations described in previous works.[15,16] To run the OPAC on JST250 the auxiliary WFS detectors are used. These detectors are grouped on pairs and distributed in 4 positions at the periphery of the JPCam focal plane mosaic. Two filters of different optical thickness are used for each WFS detector pair so a set of intra- and extra-focal images are constructed. The thickness of the auxiliary WFS filters have been estimated to introduce a de-focus equivalent to offsetting the camera focal plane by ± 1 mm. These amplitudes are a compromise between the typical size of the defocused doughnuts and their intensity. With an exposure time of 10 s, the effect of the atmospheric seeing is mostly averaged, not introducing a significant impact in the aberration determination.

From each pair of intra- and extra-focal images, the best doughnuts are selected, extracted, and analysed individually. This results in deriving the Zernike coefficients for each object at different positions of the FoV. With this information, a multi-parametric fit is done for each aberration or Zernike coefficient, hence obtaining information on the aberration and its distribution along the FoV. With it, the next step is to apply hexapod corrections to the positions of M2 and/or of the focal plane to end up with a new map of aberrations that optimizes the IQ all over the FoV. This is done through an empirical, custom made merit function.

The `OPAC` has been extensively used to operate the JAST80 telescope at the OAJ, which includes a single hexapod to control M2 position. The JST250 equipped with JPCam integrates two different hexapods, one to control M2 position and the JPCam actuator system. In this sense, the merit function used on JST250 has been significantly improved by adding a rotation matrix to the merit function, a coupling matrix to take into account the interference of the position on one hexapod to the other and changing the convergence criteria from a individual criteria for each degree of freedom to a flexible criteria that measures the expected image quality on the telescope, its uniformity and the actual seeing of the observatory.

3. COMMISSIONING AND FIRST OPERATION

The three main JPCam subsystems arrived at the OAJ at the end of 2016. These were independently accepted and commissioned, and then JPCam was fully integrated at the observatory clean room. Transportation from the clean room to the telescope and integration at the JST250 Cassegrain focus took place early 2020. In June 2020 JPCam observed the sky for the first time. Figure 8 shows the JPCam technical first light image of M31 Galaxy.

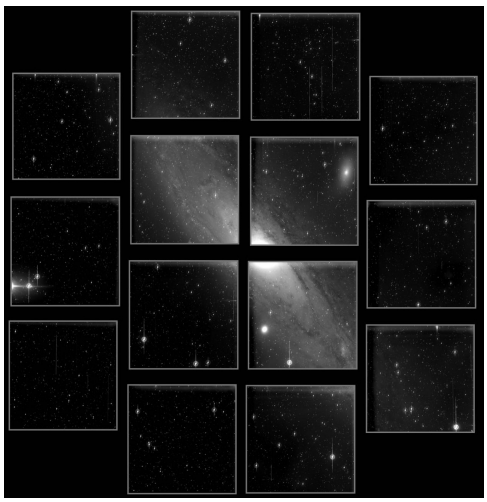

Figure 8. JPCam first light image of the Andromeda (M31) local group galaxy.

During JPCam integration at telescope and first on-sky operation, the impact of the Covid Pandemic has been significant. During the years 2020 and 2021, the activity at the OAJ was reduced to a minimum level of maintenance to guarantee the survival of the infrastructure. In this context, development activities at the observatory, including JPCam first on-sky tests, had to be postponed until the health situation allowed them to restart safely. The other main adversity JPCam commissioning is facing is related with the control CCD electronics. During the first on-sky operation of JPCam various electronics failures have been experienced on different science drive modules. Understanding the root cause of these failures has represented a challenge to the instrument team and the cryogenic camera manufacturer due to the high complexity of JPCam electronics. The failures root cause is now understood and a modification on the JPCam electronics to correct it has been designed. The implementation of the required modification is planned for the second half of 2022. For this reason, not all CCDs have been available and operative during JPCam commissioning and first operation, and this is why some of the on-sky performances and results shown in Section 4 are presented using 12 CCD images, instead of the 14 CCDs JPCam is equipped with. It is expected that all 14 scientific CCDs are available at the beginning of JPCam regular scientific operation.

4. ON-SKY PERFORMANCES

4.1 Cryogenic stability

JPCam focal plane temperature and pressure stability tests have been performed for different telescope positions, both for the elevation axis and the instrument rotator, and over a wide ambient temperature range. Cryogenic stability has been monitored during long periods of time. Results over a 10-day period are shown in Figure 9. Focal plane average temperature is controlled to a value of -112^{o}C with a variation across the focal plane (border to centre) of 1.27^{o}C (requirement is $\pm$2.5^{o}C) and a stability of 1.06^{o}C p-t-v (requirement is $\pm$0.5^{o}C). During the 10-day period shown, JPCam has been operated every night and with multiple and variable telescope elevation (from zenith to 35^o above the horizon) and instrument rotator (0^o to 360^o) orientations. The chamber pressure is maintained to a level of (1.20$\pm$0.10)$\times 10^{-9}$ Bar, well within specifications.

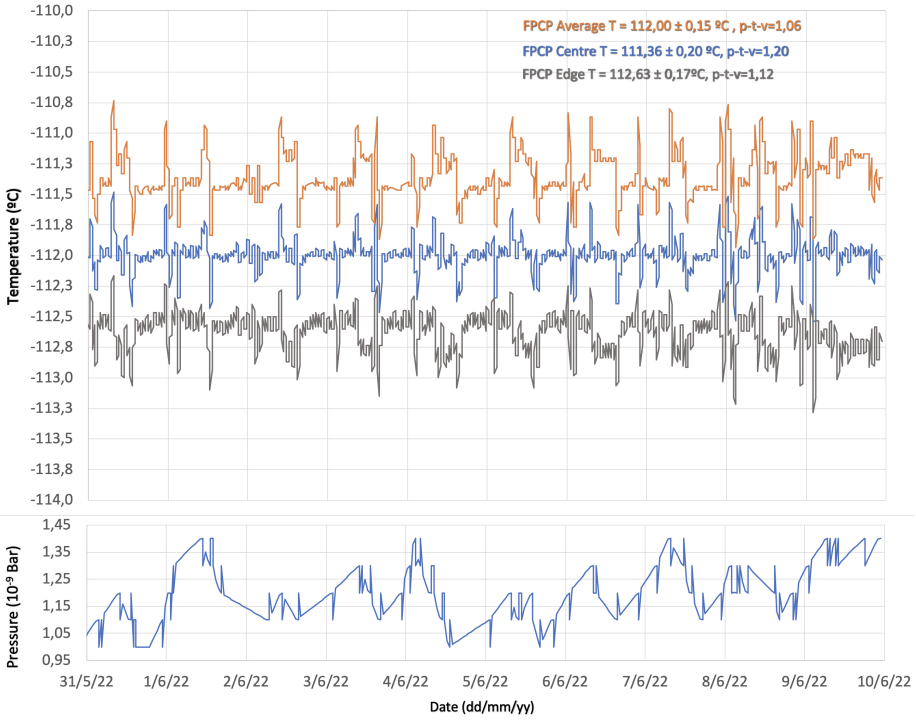

Figure 9. JPCam Focal Plane Cold Plate (FPCP) temperature and pressure stability measured over a 10 day period.

In fact, the main instability of the focal plane temperature occurs during the daily refill of the LN2 dewar. During this process, the control system optimizes the LN2 flow to minimize the impact of the LN2 refill on focal plane temperature, maintaining the temperature variation below 0.5^{o}C. It is worth mentioning that that the LN2 refill process is carried out at the beginning of the afternoon in order to ensure the focal plane temperature is back to its set value and stable during night operation.

4.2 Image quality

Image quality of large FoV telescopes and fast optics have additional challenges and tighter tolerances than conventional telescopes. Therefore, is mandatory to check the image quality of the telescope in real time and make adjustments of the positions of the secondary mirror and instrument positions. In the case of JST250 equipped with JPCam, image quality can be achieved using 3 different methods: `OPAC` with scientific CCDs, `OPAC` with M2 hexapod and JPCam actuator system Optical Control Law (OPC).

`OPAC` with scientific CCDs has been the main alignment process on commissioning, it allow us to measure directly the optical aberration on the scientific CCDs using intra- and extra-focal images. It is therefore the most accurate method but time demanding. This is the main image quality control process on JAST80. However, it has some drawbacks: the use of the scientific CCDs reduces the time available for scientific operation of the telescope and it is not possible to correct and adjust the image quality while scientific images are being taken. Once JPCam is working on regular scientific operation, this alignment process will be only applied if a system's re-calibration is needed.

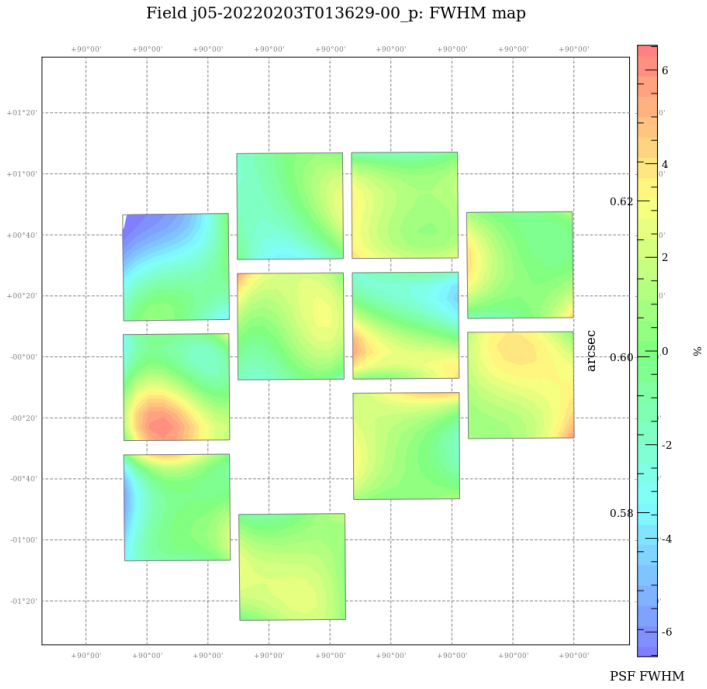

Figure 10. 2D FWHM map across JPCam FoV. Note that the two areas with FWHM $\sim 0.57''$ and $\sim 0.63''$ are a surface fitting artifact due to a border effect and low star detection density around a saturated object, respectively. Atmospheric seeing during observations was $\sim 0.55''$ FWHM.

`OPAC` with WFS CCDs. It will be the main image quality control process during and regular JPCam scientific operation. This process uses the same IQ control software, `OPAC`, but making use of the 8 WFS CCDs located

in pairs at the edges of the FoV. The use of specific CCDs to maintain IQ allow us to maximize scientific time of the telescope and the measurement and correction of the image while the telescope is taking scientific data. The drawback of this method is that indirect measurement of the optical aberration on the scientific CCDs is obtained making use of the WFS CCDs located on the periphery of the FoV, where optical aberrations of coma and astigmatism are more significant.

M2 hexapod and JPCam actuator system Optical Control Law (OPC). Every time `OPAC` with scientific CCDs is able to position the hexapod of secondary mirror and instrument with optical aberrations below the threshold of acceptable misalignment, the position of the hexapods, temperature of the telescope and and gravity vector is recorded. This database allow us to create an OCL that is able to guess with some uncertainty the optimal position of the M2 hexapod and JPCam actuator system for different pointings of the telescope. This method is almost instantaneous and provides an acceptable IQ. In particular, astigmatim aberration (related to tip/tilt of M2) is positioned with an accuracy of $1.8''$ and coma aberration (related to X-Y position of M2) is positioned with an accuracy of $17\,\mu$m. In both cases, the OCL shows enough accuracy to correct astigmatism and coma by itself. The main drawback of the OCL method is the accuracy off the correction of the defocus aberration related with Z axis of the instrument actuator and temperature changes, the accuracy of the OCL with defocus aberration is $42\,\mu$m while the IQ requirement for Z position is just $20\,\mu$m. Defocus aberration should therefore be corrected with the WFS CCDs.

During JPCam commissioning, the combination of these three methods have allow the system to maintain the position of both the M2 hexapod and JPCam actuator system with an accuracy better than the IQ and uniformity requirements. In particular, theoretical diffraction limit and as-built data gives the system JST250 and JPCam an expected IQ of $\sim 0.28''$ FWHM (without atmospheric turbulence). Real data has shown that previous methods are able to achieve IQ below $0.31''$ FWHM (without atmospheric turbulence). That is, with seeing conditions as low as $0.50''$ FWHM, the achieved JST250 and JPCam IQ is $\sim 0.59''$ and uniform along the FoV. Figure 10 shows an example of JPCam IQ during an observing run with atmospheric seeing of $\sim 0.55''$ FWHM. In cases where the seeing is $\sim 1''$ FWHM, achieved IQ is $\sim 1.05''$. The image quality of the system is therefore limited by the atmospheric seeing.

JST250 and JPCam plate scale and focal length have also beeing characterised during first on-sky operation, resulting on a plate scale value of 0.2265212 $''$/pix and a focal length of 9105.77mm, with a variation of 0.0075% between images.

Once JPCam is on regular scientific operation, IQ will be maintained with a combination of the previous methods: OCL to obtain a first order position of the M2 hexapod and actuator system, `OPAC` with WFS CCDs to maintain and correct the positions of the two hexapods while the telescope is taking scientific data, and `OPAC` with scientific CCDs on twilight to improve the accuracy of the OCL and re-calibrate scientific CCDs with WFS CCDs.

4.3 Read-out noise

The read-out noise (RON) was measured in the two read-out frequencies, 400 kHz and 630 kHz, and in full frame and 2×2 binning configurations. Sets of 10 bias with each of the four modes were acquired and the RON in electrons was computed from each consecutive pair of bias frames estimating the variance of the difference between the two: $\mathrm{RON}_{ij} = g_{ij}\,[var(\mathrm{BIAS}_{1,ij} - \mathrm{BIAS}_{0,ij})/2]^{-1/2}$, where g_{ij} is the electronic gain, in e^-/ADU, of the i-th amplifier of the j-th CCD, while $\mathrm{BIAS}_{1,ij}$ and $\mathrm{BIAS}_{0,ij}$ is the difference between the two BIAS frames in the corresponding area of the CCD. That was done for each of the 16 amplifiers of the 14 CCD.

Results are shown in Figure 11, where the mean of the measurements in each of the 4 CCD setups, 14 CCDs and 16 amplifiers are represented by a data point. The read-out noise established in the design phase as a requirement and as the goal are shown for reference too. The estimated values with the camera attached to JST250 are well bellow the requirement of $8e^-$ and much closer to the goal of $4e^-$, specially in the slow read-out speed.

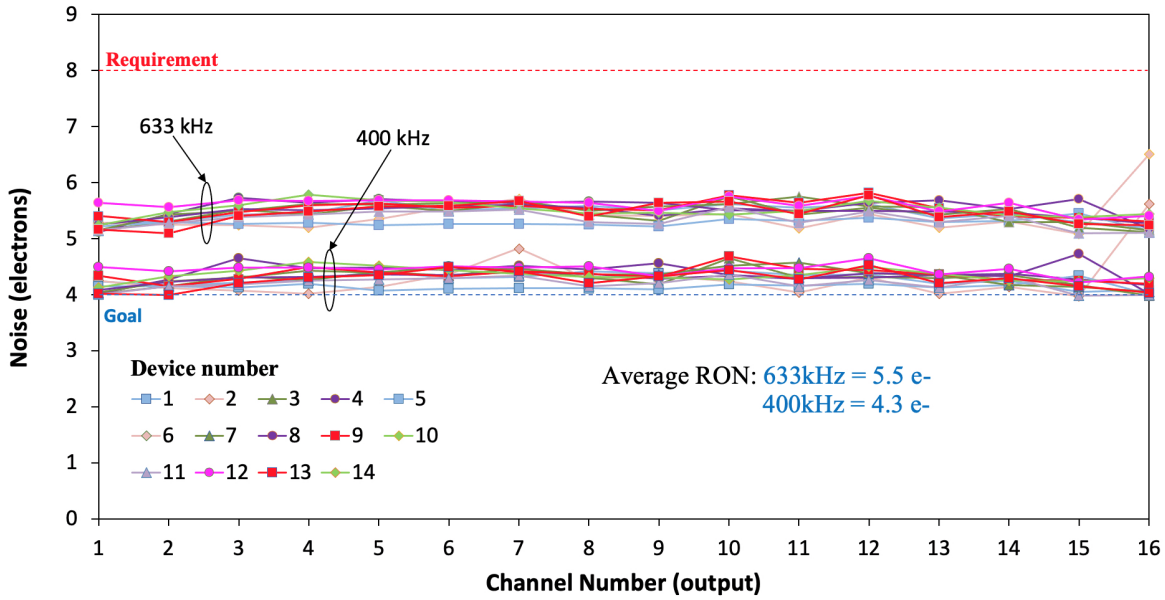

Figure 11. JPCam RON measurements. Each data point corresponds to the mean of the measurements obtained for each read-out noise, image format (full frame or binned 2×2), amplifier (from 1 to 16) and CCD device (from 1 to 14). The read-out noise level is similar under the same read-out speed. The required and desired, goal, read-out noise levels defined in the design phase are shown as well.

4.4 Zero point & limiting magnitude

The zero point (ZP) of the images, normalized to one second exposure, was estimated by comparing the instrumental magnitudes in the g band with two external references: Pan-STARRS DR2 g-band PSF magnitudes and synthetic magnitudes computed from the low-resolution *Gaia* DR3 spectra using the reference g band for J-PAS. In the process, 6 arcsec diameter aperture photometry corrected to total magnitudes for point-like objects with a photometric error lower than 0.02 mag in the JPCam images was used. The color terms between the Pan-STARRS and J-PAS g bands were evaluated and corrected. Finally, there are residual variations along the FoV that were approximated and corrected with a plane (ref?).

We analysed a set of 13 JPCam exposures, corresponding to 156 images. The median zero point obtained by comparison with Pan-STARRS was ZP $= 25.06 \pm 0.05$ mag. The zero points obtained by comparison with the *Gaia* synthetic photometry present a difference of 0.031 ± 0.003 mag with respect to those obtained with Pan-STARRS.

We estimated the zero point of the system, noted ZP_0 and defined as the magnitude of a star that produces a flux of one electron per second in the top of the atmosphere, by including the gain of the detector and the typical extinction in the g band from the OAJ. This yielded $\mathrm{ZP}_0 = 26.15 \pm 0.05$ mag. This value is close to specifications for the analyzed g band. Additional observations are needed to minimise systematics and to estimate of the zero point for the narrow bands.

The limiting magnitude of the g band calibrated images, estimated for $S/N = 5$ in a 3 arcsec diameter aperture, 60s exposure time, was $m_{\mathrm{lim}} = 23.04 \pm 0.03$ mag.

4.5 Astrometry

The astrometry is performed on each chip of the focal plane independently using Scamp[17] (v2.10.0). The radius which is used to detect reference stars is increased until a valid astrometric solution is found.For this, the parameters of the world coordinate system in the header of the images are used as a starting point. The astrometry is performed with respect to *Gaia* EDR3[18] and results in an average rms of 0.3 arcsecs.

The goodness of the astrometry was tested by cross matching against the recently issued Gaia DR3 and it is shown in Figure12. The metric that we use is the distance (in arcseconds) between the objects measured in JPCam focal plane with respect to the same objects in the Gaia DR3 catalog. The standard deviation of this distance is always larger than the mean, hence showing that the angular distance is compatible with zero. This is also always considerably smaller (about one third) of the FWHM of point sources. Across the focal plane, it is possible to see some worsening in the extreme (in particular in CCD1), whose root cause is still under investigation.

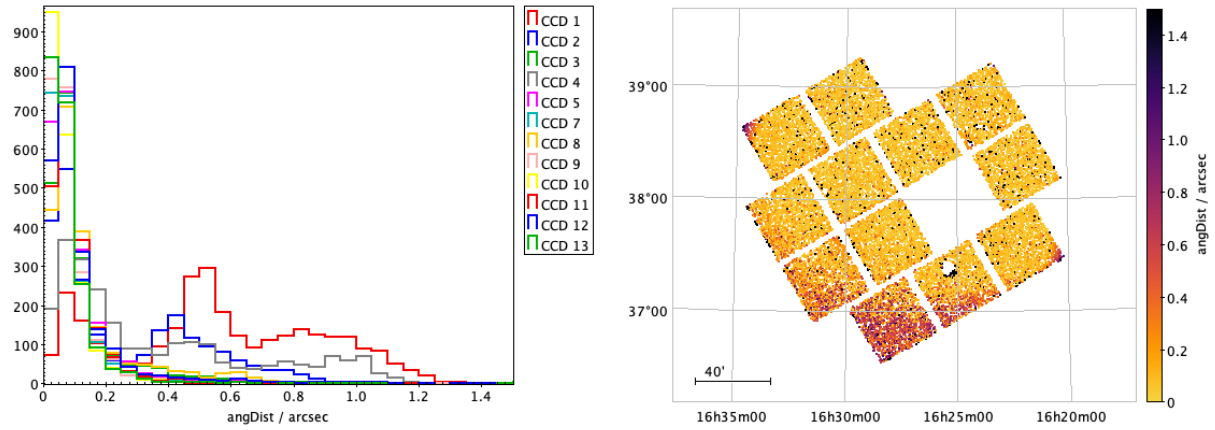

Figure 12. In the left panel, the histogram of the distance between the sources measured in the JPCam focal plane and the Gaia DR3 catalog. The different colours refer to different CCDs. In the right panel, the same distances are projected in the plane of the sky. Despite a minor increase in the southern part of the plot, the rest is remarkably uniform.

4.6 Linearity

The CCD drive modules in JPCam display good linearity at a value of over 99.95% between 5-95% of signal range. In order to test and characterize how departures from linearity can affect the photometry obtained with the JPCam, a series of tests over a battery of science images of stellar fields was performed. The images were obtained in different regions of the sky, during different nights using different exposure times ranging from 0.1 to 150 seconds in the g band. The stars observed in these runs span a wide range of magnitudes and colors, thus covering the entire dynamic range of the CCDs. We proceeded to their analysis as follow.

Aperture photometry is performed automatically for all the detected sources on each image using SExtractor. All the sources are cross-matched between the different images, grouping them based on their location in the sky. This results in a single list of sources per night, containing the photometric information for each detected object in each single image. Extended and non-stellar objects, i.e. galaxies or artifacts, are removed by selecting only sources that are also present in the Gaia DR3 catalog. We apply the criteria presented in the Gaia Early Data Release 3 (EDR3[18]) verification papers to screen out poor measurements and correct parallaxes and G magnitudes.[19,20] The final photometric list for each night contains only objects with parallax over uncertainty, $\varpi/\sigma(\varpi) > 10$, and magnitude $8 < g < 18$ mag.

For each object, the photometric list contains as many magnitude measurements as the number of images in which the object was detected. Therefore, several measurements exist for a given object and integration time. For each each object, we computed the residuals of all the magnitude measurements with respect to its median magnitude. To avoid low signal-to-noise or saturated measurements, the median was computed over the 3σ–clipped distribution of all the magnitude measurements. Upon subtraction of the median, the distribution of the residual magnitudes for each object is centered at zero. In Figure 13 we show the distribution of the residual magnitudes, measured with an aperture of 26 pixels (MAG_APER_26pix), for all the objects detected in the images corresponding to the night of 2022-05-10, as a function of the counts measured at the brightest pixel of the object's PSF (FLUX_MAX). The magnitudes of the stars are, on average, constant regardless of the number

of counts in the brightest pixel (FLUX_MAX). The saturation of the CCD is visible at FLUX_MAX $\sim$ 54000 ADU, which causes the plume of positive residual magnitudes observed on the night 2022-05-10.

Results from this tests indicate that the photometry obtained with the JPCam is linear within the entire linear range of the CCD. Furthermore, our test show that non-linearity effects can not be appreciated in the photometry along almost the entire signal range of the potential well of the CCD, even exceeding the 5%-95% range.

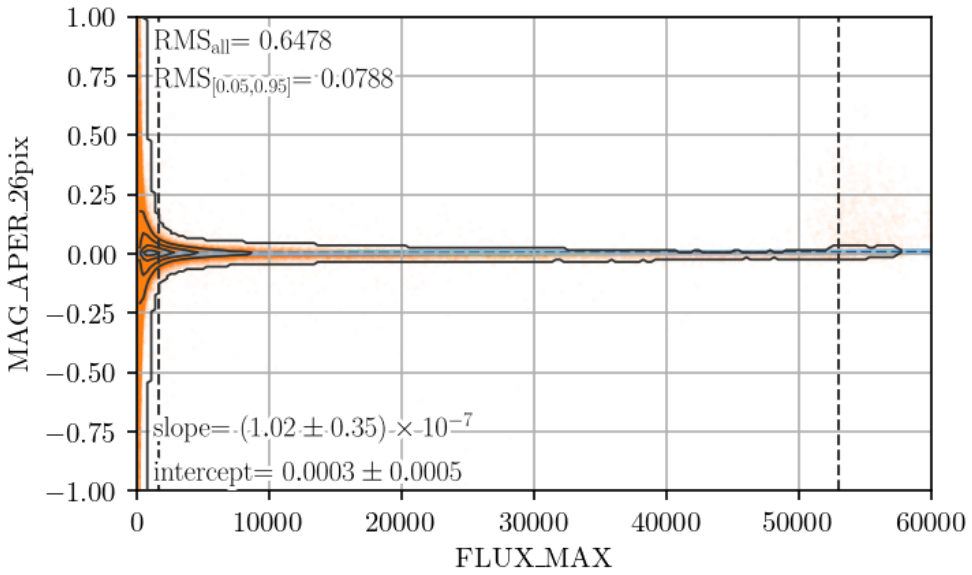

Figure 13. Linearity of the JPCam. Residual magnitudes of stellar sources measured with different integration times as a function of the flux measured at the brightest pixel of the source' PSF. Contours are in logarithmic scale and show the concentration of measurements. Vertical dashed lines indicate the 5-95% of signal range of the CCD potential well ($\sim 1500, \sim 54000$) ADUs. A linear model, fitted to the data within the 5-95% of signal range, is shown by a blue dashed line. The blue shaded area shows the model uncertainty.

ACKNOWLEDGMENTS

Based on observations made with the JST250 telescope and JPCam at the Observatorio Astrofísico de Javalambre (OAJ), in Teruel, owned, managed, and operated by the Centro de Estudios de Física del Cosmos de Aragón (CEFCA). We acknowledge the OAJ Data Processing and Archiving Unit (UPAD) for reducing and calibrating the OAJ data used in this work. Funding for the J-PAS Project has been provided by the Governments of Spain and Aragón through the Fondo de Inversión de Teruel, European FEDER funding and the Spanish Ministry of Science, Innovation and Universities, and by the Brazilian agencies FINEP, FAPESP, FAPERJ and by the National Observatory of Brazil. Additional funding was also provided by the Tartu Observatory and by the J-PAS Chinese Astronomical Consortium.

REFERENCES

[1] Benitez, N., Dupke, R., Moles, M., Sodre, L., Cenarro, J., Marin-Franch, A., Taylor, K., Cristobal, D., Fernandez-Soto, A., Mendes de Oliveira, C., Cepa-Nogue, J., Abramo, L. R., Alcaniz, J. S., Overzier, R., Hernandez-Monteagudo, C., Alfaro, E. J., Kanaan, A., Carvano, J. M., Reis, R. R. R., Martinez Gonzalez, E., Ascaso, B., Ballesteros, F., Xavier, H. S., Varela, J., Ederoclite, A., Vazquez Ramio, H., Broadhurst, T., Cypriano, E., Angulo, R., Diego, J. M., Zandivarez, A., Diaz, E., Melchior, P., Umetsu, K., Spinelli, P. F., Zitrin, A., Coe, D., Yepes, G., Vielva, P., Sahni, V., Marcos-Caballero, A., Shu Kitaura, F., Maroto, A. L., Masip, M., Tsujikawa, S., Carneiro, S., Gonzalez Nuevo, J., Carvalho, G. C., Reboucas, M. J., Carvalho,

J. C., Abdalla, E., Bernui, A., Pigozzo, C., Ferreira, E. G. M., Chandrachani Devi, N., Bengaly, C. A. P., J., Campista, M., Amorim, A., Asari, N. V., Bongiovanni, A., Bonoli, S., Bruzual, G., Cardiel, N., Cava, A., Cid Fernandes, R., Coelho, P., Cortesi, A., Delgado, R. G., Diaz Garcia, L., Espinosa, J. M. R., Galliano, E., Gonzalez-Serrano, J. I., Falcon-Barroso, J., Fritz, J., Fernandes, C., Gorgas, J., Hoyos, C., Jimenez-Teja, Y., Lopez-Aguerri, J. A., Lopez-San Juan, C., Mateus, A., Molino, A., Novais, P., OMill, A., Oteo, I., Perez-Gonzalez, P. G., Poggianti, B., Proctor, R., Ricciardelli, E., Sanchez-Blazquez, P., Storchi-Bergmann, T., Telles, E., Schoennell, W., Trujillo, N., Vazdekis, A., Viironen, K., Daflon, S., Aparicio-Villegas, T., Rocha, D., Ribeiro, T., Borges, M., Martins, S. L., Marcolino, W., Martinez-Delgado, D., Perez-Torres, M. A., Siffert, B. B., Calvao, M. O., Sako, M., Kessler, R., Alvarez-Candal, A., De Pra, M., Roig, F., Lazzaro, D., Gorosabel, J., Lopes de Oliveira, R., Lima-Neto, G. B., Irwin, J., Liu, J. F., Alvarez, E., Balmes, I., Chueca, S., Costa-Duarte, M. V., da Costa, A. A., Dantas, M. L. L., Diaz, A. Y., Fabregat, J., Ferrari, F., Gavela, B., Gracia, S. G., Gruel, N., Gutierrez, J. L. L., Guzman, R., Hernandez-Fernandez, J. D., Herranz, D., Hurtado-Gil, L., Jablonsky, F., Laporte, R., Le Tiran, L. L., Licandro, J., Lima, M., Martin, E., Martinez, V., Montero, J. J. C., Penteado, P., Pereira, C. B., Peris, V., Quilis, V., Sanchez-Portal, M., Soja, A. C., Solano, E., Torra, J., and Valdivielso, L., "J-PAS: The Javalambre-Physics of the Accelerated Universe Astrophysical Survey," *arXiv e-prints* **arXiv:1403.5237**, arXiv:1403.5237 (Mar. 2014).

[2] Bonoli, S., Marín-Franch, A., Varela, J., Vázquez Ramió, H., Abramo, L. R., Cenarro, A. J., Dupke, R. A., Vílchez, J. M., Cristóbal-Hornillos, D., González Delgado, R. M., Hernández-Monteagudo, C., López-Sanjuan, C., Muniesa, D. J., Civera, T., Ederoclite, A., Hernán-Caballero, A., Marra, V., Baqui, P. O., Cortesi, A., Cypriano, E. S., Daflon, S., de Amorim, A. L., Díaz-García, L. A., Diego, J. M., Martínez-Solaeche, G., Pérez, E., Placco, V. M., Prada, F., Queiroz, C., Alcaniz, J., Alvarez-Candal, A., Cepa, J., Maroto, A. L., Roig, F., Siffert, B. B., Taylor, K., Benitez, N., Moles, M., Sodré, L., Carneiro, S., Mendes de Oliveira, C., Abdalla, E., Angulo, R. E., Aparicio Resco, M., Balaguera-Antolínez, A., Ballesteros, F. J., Brito-Silva, D., Broadhurst, T., Carrasco, E. R., Castro, T., Cid Fernandes, R., Coelho, P., de Melo, R. B., Doubrawa, L., Fernandez-Soto, A., Ferrari, F., Finoguenov, A., García-Benito, R., Iglesias-Páramo, J., Jiménez-Teja, Y., Kitaura, F. S., Laur, J., Lopes, P. A. A., Lucatelli, G., Martínez, V. J., Maturi, M., Overzier, R. A., Pigozzo, C., Quartin, M., Rodríguez-Martín, J. E., Salzano, V., Tamm, A., Tempel, E., Umetsu, K., Valdivielso, L., von Marttens, R., Zitrin, A., Díaz-Martín, M. C., López-Alegre, G., López-Sainz, A., Yanes-Díaz, A., Rueda-Teruel, F., Rueda-Teruel, S., Abril Ibañez, J., L Antón Bravo, J., Bello Ferrer, R., Bielsa, S., Casino, J. M., Castillo, J., Chueca, S., Cuesta, L., Garzarán Calderaro, J., Iglesias-Marzoa, R., Íniguez, C., Lamadrid Gutierrez, J. L., Lopez-Martinez, F., Lozano-Pérez, D., Maícas Sacristán, N., Molina-Ibáñez, E. L., Moreno-Signes, A., Rodríguez Llano, S., Royo Navarro, M., Tilve Rua, V., Andrade, U., Alfaro, E. J., Akras, S., Arnalte-Mur, P., Ascaso, B., Barbosa, C. E., Beltrán Jiménez, J., Benetti, M., Bengaly, C. A. P., Bernui, A., Blanco-Pillado, J. J., Borges Fernandes, M., Bregman, J. N., Bruzual, G., Calderone, G., Carvano, J. M., Casarini, L., Chaves-Montero, J., Chies-Santos, A. L., Coutinho de Carvalho, G., Dimauro, P., Duarte Puertas, S., Figueruelo, D., González-Serrano, J. I., Guerrero, M. A., Gurung-López, S., Herranz, D., Huertas-Company, M., Irwin, J. A., Izquierdo-Villalba, D., Kanaan, A., Kehrig, C., Kirkpatrick, C. C., Lim, J., Lopes, A. R., Lopes de Oliveira, R., Marcos-Caballero, A., Martínez-Delgado, D., Martínez-González, E., Martínez-Somonte, G., Oliveira, N., Orsi, A. A., Penna-Lima, M., Reis, R. R. R., Spinoso, D., Tsujikawa, S., Vielva, P., Vitorelli, A. Z., Xia, J. Q., Yuan, H. B., Arroyo-Polonio, A., Dantas, M. L. L., Galarza, C. A., Gonçalves, D. R., Gonçalves, R. S., Gonzalez, J. E., Gonzalez, A. H., Greisel, N., Jiménez-Esteban, F., Landim, R. G., Lazzaro, D., Magris, G., Monteiro-Oliveira, R., Pereira, C. B., Rebouças, M. J., Rodriguez-Espinosa, J. M., Santos da Costa, S., and Telles, E., "The miniJPAS survey: A preview of the Universe in 56 colors," *Astronomy & Astrophysics* **653**, A31 (Sept. 2021).

[3] Cenarro, A. J., Moles, M., Marín-Franch, A., Cristóbal-Hornillos, D., Yanes Díaz, A., Ederoclite, A., Varela, J., Vázquez Ramió, H., Valdivielso, L., Benítez, N., Cepa, J., Dupke, R., Fernández-Soto, A., Mendes de Oliveira, C., Sodré, L., Taylor, K., Rueda-Teruel, S., Rueda-Teruel, F., Luis-Simoes, R., Chueca, S., Antón, J. L., Bello, R., Díaz-Martín, M. C., Guillén-Civera, L., Hernández-Fuertes, J., Iglesias-Marzoa, R., Jiménez-Mejías, D., Lasso-Cabrera, N. M., López-Alegre, G., López-Sainz, A., Rodríguez-Hernández, M. A. C., Suárez, O., Lamadrid, J. L., Maícas, N., Abril-Ibañez, J., Tilve, V., and Rodríguez-Llano, S., "The Observatorio Astrofísico de Javalambre: current status, developments, operations, and strategies," in [*Observatory Operations: Strategies, Processes, and Systems V*], Peck, A. B., Benn, C. R., and Seaman,

R. L., eds., *Society of Photo-Optical Instrumentation Engineers (SPIE) Conference Series* **9149**, 91491I (Aug. 2014).

[4] Moles, M., Sánchez, S. F., Lamadrid, J. L., Cenarro, A. J., Cristóbal-Hornillos, D., Maicas, N., and Aceituno, J., "Site Testing of the Sierra de Javalambre: First Results," *Publications of the Astronomical Society of the Pacific* **122**, 363 (Mar. 2010).

[5] Cristóbal-Hornillos, D., Varela, J., Ederoclite, A., Vázquez Ramió, H., López-Sainz, A., Hernández-Fuertes, J., Civera, T., Muniesa, D., Moles, M., Cenarro, A. J., Marín-Franch, A., and Yanes-Díaz, A., "Data management pipeline and hardware facilities for J-PAS and J-PLUS surveys archiving and processing," in [*Software and Cyberinfrastructure for Astronomy III*], Chiozzi, G. and Radziwill, N. M., eds., *Society of Photo-Optical Instrumentation Engineers (SPIE) Conference Series* **9152**, 91520O (July 2014).

[6] Cenarro, A. J., Ederoclite, A., Íñiguez, C., Marín-Franch, A., Vázquez Ramió, H., Yanes-Díaz, A., Chueca, S., Lasso-Cabrera, N. M., Rueda-Teruel, S., Rueda-Teruel, F., Cristóbal-Hornillos, D., Varela, J., López-Alegre, G., Bello, R., Antón-Bravo, J. L., Bielsa de Toledo, S., Domínguez-Martínez, M., Moreno-Signes, A., Iglesias-Marzoa, R., Díaz-Martín, M. C., Civera, T., Hernández-Fuertes, J., Muniesa-Gallardo, D., Castillo, J., López-Sáinz, A., Moles, M., Lousberg, G. P., Bastin, C., and Pirnay, O., "Commissioning and first scientific operations of the wide-field 2.6m Javalambre Survey Telescope," in [*Ground-based and Airborne Telescopes VII*], Marshall, H. K. and Spyromilio, J., eds., *Society of Photo-Optical Instrumentation Engineers (SPIE) Conference Series* **10700**, 107000D (July 2018).

[7] Taylor, K., Marín-Franch, A., Laporte, R., Santoro, F. G., Marrara, L., Cepa, J., Cenarro, A. J., Chueca, S., Cristobal-Hornillos, D., Ederoclite, A., Gruel, N., Moles, M., Rueda, F., Rueda, S., Varela, J., Yanes, A., Benitez, N., Dupke, R., Fernández-Soto, A., Jorden, P., Lousberg, G., Molino Benito, A., Palmer, I., Mendes de Oliveira, C., and Sodré, L., "Jpcam: a 1.2 Gpixel Camera for the J-Pas Survey," *Journal of Astronomical Instrumentation* **3**, 1350010–685 (Mar. 2014).

[8] Marín-Franch, A., Taylor, K., Santoro, F. G., Laporte, R., Cepa, J., Lasso-Cabrera, N., Yanes-Díaz, A., Cenarro, A. J., Cristobal-Hornillos, D., Ederoclite, A., Moles, M., Varela, J., Vázquez Ramió, H., Antón, J. L., Bello, R., Civera, T., Castillo, J., Chueca, S., Guillén-Civera, L., Hernández-Fuertes, J., Igual, R., Íniguez, C., López-Alegre, G., López-Sainz, A., Nevot, C., Milla, R., Muniesa, D., Pe, A., Rueda-Teruel, R., Rueda-Teruel, F., Sánchez, J., Benitez, N., Dupke, R., Fernández-Soto, A., Mendes de Oliveira, C., and Sodré, L., "JPCam: Development of a 1.2 Gpixel Camera for the J-PAS Survey," in [*Highlights on Spanish Astrophysics IX*], Arribas, S., Alonso-Herrero, A., Figueras, F., Hernández-Monteagudo, C., Sánchez-Lavega, A., and Pérez-Hoyos, S., eds., 670–675 (Mar. 2017).

[9] Chueca, S., Marín-Franch, A., Cenarro, A. J., Varela, J., Ederoclite, A., Cristóbal-Hornillos, D., Hernández-Monteagudo, C., Gruel, N., Moles, M., Yanes, A., Rueda, F., Rueda, S., Luis-Simoes, R., Hernández-Fuertes, J., López-Sainz, A., Maícas-Sacristán, N., Lamadrid, J. L., Díaz-Martín, M. C., and Taylor, K., "Curvature wavefront sensing performance simulations for active correction of the Javalambre wide-field telescopes," in [*Modern Technologies in Space- and Ground-based Telescopes and Instrumentation II*], Navarro, R., Cunningham, C. R., and Prieto, E., eds., *Society of Photo-Optical Instrumentation Engineers (SPIE) Conference Series* **8450**, 84500I (Sept. 2012).

[10] Robbins, M. S., Bastable, M., Bates, A., Dryer, M., Eames, S., Fenemore-Jones, G., Haddow, G., Jorden, P. R., Lane, B., Marin-Franch, A., Mortimer, J., Palmer, I., Puttay, N., Renshaw, R., Smith, M., Taylor, K., Tearle, J., Weston, P., Wheeler, P., and Worley, J., "Performance of the e2v 1.2 GPix cryogenic camera for the J-PAS 2.5m survey telescope," in [*Ground-based and Airborne Instrumentation for Astronomy VI*], Evans, C. J., Simard, L., and Takami, H., eds., *Society of Photo-Optical Instrumentation Engineers (SPIE) Conference Series* **9908**, 990811 (Aug. 2016).

[11] Marín-Franch, A., Chueca, S., Moles, M., Benitez, N., Taylor, K., Cepa, J., Cenarro, A. J., Cristobal-Hornillos, D., Ederoclite, A., Gruel, N., Hernández-Fuertes, J., López-Sainz, A., Luis-Simoes, R., Rueda-Teruel, F., Rueda-Teruel, S., Varela, J., Yanes-Díaz, A., Brauneck, U., Danielou, A., Dupke, R., Fernández-Soto, A., Mendes de Oliveira, C., and Sodré, L., "Design of the J-PAS and J-PLUS filter systems," in [*Modern Technologies in Space- and Ground-based Telescopes and Instrumentation II*], Navarro, R., Cunningham, C. R., and Prieto, E., eds., *Society of Photo-Optical Instrumentation Engineers (SPIE) Conference Series* **8450**, 84503S (Sept. 2012).

[12] Brauneck, U., Sprengard, R., Bourquin, S., and Marín-Franch, A., "Customized broadband Sloan-filters for the JST/T250 and JAST/T80 telescopes: measurement summary," *Journal of Astronomical Telescopes, Instruments, and Systems* **4**, 015002 (Jan. 2018).

[13] Brauneck, U., Sprengard, R., Bourquin, S., and Marín-Franch, A., "Dense grid of narrow bandpass filters for the JST/T250 telescope: summary of results," *Journal of Astronomical Telescopes, Instruments, and Systems* **4**, 015003 (Jan. 2018).

[14] Casalta, J. M., Canchado, M., Molins, A., Redondo, M., Tomàs, A., and Catalan, A., "Design and performances of JPCam actuator system," in [*Advances in Optical and Mechanical Technologies for Telescopes and Instrumentation*], *Proc. SPIE* **9151**, 915109 (July 2014).

[15] Noll, R. J., "Zernike polynomials and atmospheric turbulence," *JOsA* **66**(3), 207–211 (1976).

[16] Roddier, C. and Roddier, F., "Wave-front reconstruction from defocused images and the testing of ground-based optical telescopes," *JOSA A* **10**(11), 2277–2287 (1993).

[17] Bertin, E., "Automatic Astrometric and Photometric Calibration with SCAMP," in [*Astronomical Data Analysis Software and Systems XV*], Gabriel, C., Arviset, C., Ponz, D., and Enrique, S., eds., *Astronomical Society of the Pacific Conference Series* **351**, 112 (July 2006).

[18] Gaia Collaboration, "Gaia early data release 3 - summary of the contents and survey properties," *A&A* **649**, A1 (2021).

[19] Lindegren, L., Bastian, U., Biermann, M., Bombrun, A., de Torres, A., Gerlach, E., Geyer, R., Hernández, J., Hilger, T., Hobbs, D., Klioner, S. A., Lammers, U., McMillan, P. J., Ramos-Lerate, M., Steidelmüller, H., Stephenson, C. A., and van Leeuwen, F., "Gaia Early Data Release 3. Parallax bias versus magnitude, colour, and position," *A&A* **649**, A4 (May 2021).

[20] Riello, M., De Angeli, F., Evans, D. W., Montegriffo, P., Carrasco, J. M., Busso, G., Palaversa, L., Burgess, P. W., Diener, C., Davidson, M., Rowell, N., Fabricius, C., Jordi, C., Bellazzini, M., Pancino, E., Harrison, D. L., Cacciari, C., van Leeuwen, F., Hambly, N. C., Hodgkin, S. T., Osborne, P. J., Altavilla, G., Barstow, M. A., Brown, A. G. A., Castellani, M., Cowell, S., De Luise, F., Gilmore, G., Giuffrida, G., Hidalgo, S., Holland, G., Marinoni, S., Pagani, C., Piersimoni, A. M., Pulone, L., Ragaini, S., Rainer, M., Richards, P. J., Sanna, N., Walton, N. A., Weiler, M., and Yoldas, A., "Gaia early data release 3 - photometric content and validation," *A&A* **649**, A3 (2021).